



Universidad del País Vasco  
Euskal Herriko Unibertsitatea



ZTF-FCT  
Zientzia eta Teknologia Fakultatea  
Facultad de Ciencia y Tecnología



---

FACULTY OF SCIENCE AND TECHNOLOGY. LEIOA

---

# UNDERGRADUATE RESEARCH PROJECT BIOCHEMISTRY AND MOLECULAR BIOLOGY

---

## STUDY ON THE ACTIVATION MECHANISM OF BCL-2 RELATED OVARIAN KILLER (BOK)

**Student:** *Goya Grocin, Andrea*

**Date:** June 2015

**Directors:**

*Dr. Olatz Landeta Diaz*

*Dr. Oihana Terrones Urio*

**Academic year**

2014/15

# INDEX

	<u>Page</u>
<b>1. Introduction and Main Objectives</b> .....	<b>1</b>
<b>2. Materials and Methods</b> .....	<b>3</b>
2.1. Mutagenesis of GST-BOK $\Delta$ C-6His.....	<b>3</b>
2.2. Transformation of <i>E. coli</i> DH5 $\alpha$ competent cells.....	<b>4</b>
2.3. Extraction of the amplified DNA plasmid.....	<b>4</b>
2.4. Expression of GST-BOK $\Delta$ C-6His in several <i>E. coli</i> strains.....	<b>4</b>
2.5. Purification of GST-BOK $\Delta$ C-6His.....	<b>4</b>
2.5.1. Cell disruption and lysate clearance.....	<b>4</b>
2.5.2. Affinity purification.....	<b>5</b>
2.5.3. Size-exclusion chromatography.....	<b>5</b>
2.6. Liposome preparation.....	<b>5</b>
2.7. Tryptophan fluorescence assays.....	<b>6</b>
2.8. ANTS/DPX leakage fluorescence assay.....	<b>6</b>
<b>3. Results</b> .....	<b>6</b>
3.1. Mutagenesis of GST-BOK $\Delta$ C-6His.....	<b>6</b>
3.2. Expression of recombinant GST-BOK $\Delta$ C-6His.....	<b>7</b>
3.3. Purification of GST-BOK $\Delta$ C-6His WT and mutants.....	<b>8</b>
3.4. Tryptophan fluorescence assays.....	<b>10</b>
3.5. ANTS/DPX release fluorescence assays.....	<b>11</b>
<b>4. Discussion</b> .....	<b>12</b>
<b>5. Concluding Remarks</b> .....	<b>14</b>
<b>6. References</b> .....	<b>14</b>

## 1. INTRODUCTION AND MAIN OBJECTIVES

Apoptosis or programmed cell death is a controlled sequential process that is essential for normal embryonic development and healthy tissue homeostasis. In fact, excessive apoptosis can lead to several illnesses including neurodegenerative diseases and AIDS, whereas reduced apoptosis is key in cancer (1,2).

With such important roles, apoptosis must be –and in fact, is– a tightly controlled process. The tripartite B-cell lymphoma-2 (BCL-2) family is widely recognized as the main protein family regulating the mitochondrial outer membrane (MOM) permeabilization (MOMP), which has been described as the point of no return in the intrinsic (mitochondrial) pathway of apoptosis (3,4). This process leads to the release of cytochrome c and other apoptogenic factors (AIF, Smac/DIABLO...) from the intermembrane space to the cytosol resulting in caspase activation (5).

Depending on functional criteria and on their content in BCL-2 homology (BH) domain sequences, proteins of the BCL-2 family are classified into three subgroups: [i] the pro-survival or anti-apoptotic multi-domain proteins (BCL-2, BCL-X<sub>L</sub> and others), which contain up to four BH domains and inhibit MOMP; [ii] the pro-apoptotic multi-domain or BAX-like proteins (BAX, BAK and most probably, BOK), which once activated gain pore-forming activity permeabilizing the MOM and [iii] the pro-apoptotic BH3-only proteins (BIM, tBID and others), which possess just the BH3 domain and trigger functional activation of BAX-like proteins either directly or indirectly (2,6).

BCL-2 related Ovarian Killer (BOK) displays ~70-80% sequence homology to BAX and BAK, sharing its BH1-3 domains and a C-terminal transmembrane domain (7,8). Moreover, it has been reported to permeabilize both liposomal models and mitochondria as well as to induce cell death upon transient overexpression (7). All this evidence has raised the possibility that BOK could be a BAX-like BCL-2 family member (6–8).

However, unlike BAX and BAK, little is known about BOK. It was initially reported to be in reproductive tissues, but more recent studies showed it can be detected in most tissues (6). Attention has been drawn to the fact that the *Bok* gene is localized in a genomic region that is frequently deleted in human cancer, raising the question whether it acts as a tumour suppressor (9). Nevertheless, this idea seems to be inconsistent with the fact that *Bok* KO mice appear to develop normally and *Bok*<sup>-/-</sup> hematopoietic respond normally to various classical apoptotic stimuli (6,7). Interestingly, BOK has been reported to induce apoptosis only in the presence of BAX and BAK, as overexpression of BOK could not kill *Bax*<sup>-/-</sup> *Bak*<sup>-/-</sup> doubly deficient cells (6), which seems to indicate that BOK acts upstream BAX and BAK (7). This, however, cannot explain why *Bok* KO mice and hematopoietic cells developed and responded normally.

More recently, BOK has been shown to be important for ER stress responses, driven by the fact that BOK localizes to the ER and Golgi in addition to the MOM (6,7). Nonetheless, BAX and BAK have been reported to localize to those cellular compartments as well (6), which means a mitochondrial role for BOK cannot be ruled out either.

The structure of BOK has not been solved yet but it presumably has a similar 3D structure to BAX-like proteins (2): a helical bundle structure composed by a total of nine alpha-helices ( $\alpha 1 - \alpha 9$ ) being the C-terminal  $\alpha 9$  helix a transmembrane domain. This fold delineates a hydrophobic groove ( $\alpha 3 - \alpha 5$ ) that has been proposed to constitute a crucial interface for interactions with other BCL-2 pro-apoptotic members via their BH3-domain (2).

BAX and BAK have been reported to activate and oligomerize upon activation of certain BH3-only proteins (activators) such as BID and BIM binding to their canonical hydrophobic groove (10,11). This oligomerization seems to be essential for MOM permeabilization or MOMP resulting in cytochrome c release and subsequent cell death.

One main model has been proposed for BAX (12) and BAK (10) activation. In this model, when an activator BH3-only protein transiently inserts its BH3 helical domain into the hydrophobic canonical groove (helices  $\alpha 3 - \alpha 5$ ) of the pro-apoptotic protein (10,12), the core domain ( $\alpha 2 - \alpha 5$  and probably  $\alpha 1$ ) is released from the latch domain ( $\alpha 6 - \alpha 8$ ). This structural rearrangement frees the BH3 helical domain ( $\alpha 2$ ), which is now able to compete for the groove of another BAX protein (10,12). Indeed, the crystal structure showed an homodimer in which the BH3-only helix of one BAX/BAK monomer was inserted into the hydrophobic groove of the other one in a symmetrical fashion (10,12). This dimerization model has been further supported by several biochemical and biophysical studies (13–15) and seems to be a key event in the oligomerization process, although how BAX/BAK dimers interact to form the apoptotic pore remains unclear despite new studies in the field (16). This could be due to the formation of a proteolipidic pore (1,17,18), which could hinder its structural analysis.

Further characterization of the BH3-in-groove homodimer in BAK and BAX has shown some key interaction that hold the two monomers together. Particularly important are five hydrophobic residues (h0 – h4) in the BH3 domain and a salt bridge formed between an Asp residue in the BH3 domain and an arginine in  $\alpha 5$  helix (hydrophobic groove) (2,10,12). In fact, a non-conserved mutation of the R109 in BAX (corresponding to K122 in BOK) has been reported to abrogate dimerization (12).

Although BOK having been proposed to have a similar structure to BAX and BAK, its activation has not been studied yet, being unclear if it dimerizes the way BAX-like proteins do. Thus, the **aim** of this research project is to unravel the membrane activity of BOK; test whether BOK forms a dimer following the same BH3-in-groove model as BAX and BAK in order to gain their pore-forming activity.

In order to determine whether BOK follows the BH3-in-groove dimerization mechanism of its pro-apoptotic relatives, two different mutants were designed –D75R, in the BH3 domain ( $\alpha 2$ ) and K122E, in the canonical hydrophobic groove ( $\alpha 5$ )–, which predictably disrupted the proposed model of interaction as they correspond to the residues forming a key salt-bridge in the BH3-in-groove homodimer of BAK and BAX (5,7). Therefore, these mutations were hypothesized to ablate BOK’s pore-forming activity, for which dimerization was predicted to be necessary. In this project, D75R and K122E mutants were generated, expressed and tested for union and pore-forming activity on liposomal models of the MOM.

The **main limitation** linked to this experiment is the generation and expression of the mutants, which can differ from those of the WT protein both in experimental conditions and yield. Furthermore, this approach will just give us a glimpse of the real BOK activation mechanisms, which should be further investigated in a more physiological-like environment such as isolated mitochondrial membrane vesicles (OMVs), isolated mitochondria or even cell-level studies.

## 2. METHODS

### 2.1. MUTAGENESIS OF GST-BOK $\Delta$ C-6HIS

The starting point was an *Escherichia coli* codon optimized, GST-tagged BOK construct inserted into a pGEX-3p-6 vector plasmid. This BOK sequence lacked the last 24 amino acids corresponding to its transmembrane domain at its C-terminus in order to ease its manipulation in bacterial culture. In addition to a GST tag in its N-terminus followed by a PreScission protease cleavage site (LEVLFQ/GP), it also had a 6-histidine tag at its C-terminus.

The GST-BOK $\Delta$ C-6His construct was subjected to a mutagenic PCR using the Quick Change® Site-Directed Mutagenesis Kit (Agilent Technologies, CA, USA). The following primers were used: forward 5'-GTTCTGCTGCGCCTGGGTCGCGAATTGGAGATG-3' and reverse 5'-CATCTCCAA TTCGCGACCCAGGCGCAGCAGAAC-3' to obtain a D75R mutant and forward 5'-GTATCACGT GGGGCGAGGTCGTTAGCCTG-3' and reverse 5'-CAGGCTAACGACCTCGCCCCACGTGATAC-3' to obtain a K122E mutant. All primers used were synthetically synthesized by Sigma Aldrich (Madrid, Spain) and had a  $T_m \geq 79.4$  °C and a GC content of 60-62%. Each sample was prepared as indicated in the kit’s user’s manual (1 ng/ $\mu$ L construct template, 2.5 ng/ $\mu$ L of each primer, 5  $\mu$ L 10x reaction buffer, 20 mM DNTP mix, 2.5 U Pfu Turbo DNA polymerase and ddH<sub>2</sub>O to a total of 50  $\mu$ L). The PCR conditions were set as follows:

Step	Temperature	Time	Cycles
Denaturation	95 °C	30 seconds	1
Denaturation	95 °C	30 seconds	
Annealing	55 °C	1 minute	20
Extension	72 °C	5 minutes	
Extension	72 °C	10 minutes	1

The PCR product was then incubated for 1 h at 37°C in the presence of Dpn I endonuclease, which degrades the parental methylated DNA template allowing for selection of mutation-containing newly synthesized DNA.

## **2.2. TRANSFORMATION OF *E. coli* DH5 $\alpha$ COMPETENT CELLS**

All PCR product was added to 50  $\mu$ L *E. coli* competent cells. Cells were first incubated on ice for 30 min. Then, cells were heat-shocked for 90 s at 42 °C to form transient pores through which the added DNA enters the cells. Cells were allowed to recover on ice for another 30 min. Subsequently, 1 mL Luria Broth (LB) medium was added to the mixture and incubated with gentle stirring for 1 h at 37 °C. Next, cells were spun down in a benchtop centrifuge at 8,000 x g for 1 min; the supernatant was discarded and the pellet was resuspended on 50  $\mu$ L of LB medium. Finally, cells were plated in ampicillin containing agar plates and incubated at 37 °C overnight. Vector containing colonies were selected on ampicillin containing agar.

## **2.3. EXTRACTION OF THE AMPLIFIED DNA PLASMID**

Several colonies were randomly picked from the agar plate and grown overnight in 10 mL of LB containing ampicillin (100  $\mu$ g/mL). The DNA plasmid was then isolated by alkaline cell disruption and further plasmid purification using a QIAprep Spin Miniprep Kit (Qiagen, California, USA) and following manufacturer's instructions. DNA concentration (absorbance at 260 nm,  $A_{260}$ ) and purity ( $A_{260}/A_{280}$  ratio) was determined via Nanodrop<sup>TM</sup> (Thermo Scientific, Waltham, MA, USA). Aliquots from each colony plasmid purification were checked for the corresponding mutations by sequencing (Secugen S.L., Madrid, Spain).

## **2.4. EXPRESSION OF GST-BOK-6HIS IN SEVERAL *E. coli* STRAINS**

Transformation of *E. coli* cells was performed as explained in **section 2.2**. Several colonies were picked and placed into 10 mL of LB medium containing ampicillin (100  $\mu$ g/mL). Cells were incubated in an orbital shaker at 37 °C overnight. Next morning, the cell culture was escalated by placing 1 mL aliquot into 100 mL of LB medium containing ampicillin and then into 1 L medium in a stepwise manner. Cells were cultured in an orbital shaker at 37 °C until an optical density ( $OD_{600\text{ nm}}$ ) of 1 was reached. Then, protein expression was induced by adding isopropyl  $\beta$ -D-thiogalactopyranoside (IPTG) and cells were cultured in an orbital shaker for 18 h at 20 °C. Lastly, bacteria were collected by centrifugation at 5,000 x g for 30 min at 4°C in a Beckman Coulter centrifuge using a JLA-9.100 rotor (Beckman Coulter, Fullerton, California, USA). The pellet was stored at -80°C.

## **2.5. PURIFICATION OF GST-BOK $\Delta$ C-6HIS**

### **2.5.1. Cell disruption and lysate clearance**

Bacterial pellets were resuspended in Buffer A (500 mM NaCl, 20 mM Tris, 1mM EDTA, 40 mM mercaptoethanol, 20% glycerol; pH 8.0) supplemented with freshly prepared 1 mg/mL lysozyme (Sigma-Aldrich), bacterial protein inhibitors (Roche, Basel, Switzerland) and 2.5 µg/mL DNase (Sigma-Aldrich). Cells were then homogenized at 17,000 psi in a high-pressure Emulsiflex-C5 homogenizer (Avestin, ON, Canada) in order to avoid protein aggregation caused by sonication. The resultant cell lysate suspension was centrifuged at 20,000 x g for 30 min at 4 °C. The supernatant was kept at 4°C for subsequent steps.

### **2.5.2. Affinity purification**

A first purification step was performed using a column containing Glutathione Sepharose 4B beads (GE Healthcare). For each pellet coming from 2 L of bacterial culture 1 mL of washed glutathione beads was required. The bacterial supernatant was then mixed with the beads and the mixture was incubated in an orbital rotator for 2 h at 4 °C to allow glutathione S-transferase in the recombinant proteins to bind the reduced glutathione beads.

The beads with bound protein were then packed into a column connected to a peristaltic pump. After addition of five bead-volumes of Buffer A, 60 U of PreScission protease (GE Healthcare, Waukesha, WI, USA) was added. The column was then sealed and stored at 4 °C overnight to allow efficient protease cleavage. Next morning, the cleaved protein was eluted from the column using Buffer B (500 mM NaCl, 20 mM Bis-Tris, 1mM EDTA, 40 mM mercaptoethanol, 20% glycerol; pH 6.0) in 0.5 mL fractions, which were collected for SDS-PAGE analysis and Coomassie blue staining, as well as Western blotting.

### **2.5.3. Size-Exclusion Chromatography**

Fractions containing BOKΔC-6His were pooled and loaded onto a Superdex™ 75 size exclusion column previously equilibrated with Buffer B. Elution was performed at 0.3 mL/min flow-rate, at 4°C and followed by monitoring UV absorbance at 280 nm and 254 nm. The sample was collected in fractions of 0.5 mL for subsequent SDS-PAGE analysis and Coomassie blue staining.

## **2.6. LIPOSOME PREPARATION**

Liposomes were prepared with two lipid composition 85 PC/15 CL (15% CL) and 100 CL (100% CL) (% mol/mol). Lipid mixtures at the indicated ratios were co-dissolved in chloroform/methanol (2:1), and organic solvent was removed by evaporation under a nitrogen stream followed by incubation under vacuum for 2 h. Dry lipid films were resuspended in 100 mM KCl, 10 mM HEPES pH 7.0 and 0.1 mM EDTA (KHE buffer). For membrane permeabilization assays, KHE buffer was supplemented with 12.5 mM ANTS and 45 mM DPX. Multilamellar vesicles were next subjected to 10 freeze/thaw cycles and were then extruded 10 times through two polycarbonate membranes of 0.1 µm pore-size

(Nucleopore, San Diego, CA) to obtain large unilamellar vesicles (LUVs). Untrapped ANTS/DPX was removed by gel filtration in a PD10-desalting column with KHE as elution buffer.

## 2.7. TRYPTOPHAN FLUORESCENCE ASSAYS

BOK $\Delta$ C-6His WT and D75R mutant intrinsic fluorescence emission spectra were monitored in the absence or presence of LUVs. Proteins (500 nM) were incubated with or without LUVs (500  $\mu$ M) for 10 min prior to the beginning of the measurements. Fluorescence spectra were recorded using a SLM 8100 photon-counting spectrofluorometer (Spectronic Instrument, Rochester, NY, USA) with an excitation wavelength of 295 nm (5 nm band pass) and measuring emission spectra from 300 nm to 450 nm (5 nm band pass) at a rate of 1 nm/s with the experiment conducted at 37°C. The contribution of the buffer or liposomes alone was subtracted as blank and the fluorescence intensity maximum was normalized to 1 in order to facilitate peak wavelength comparison.

## 2.8. ANTS/DPX LEAKAGE FLUORESCENCE ASSAY

The polyanionic fluorophore 8-aminonaphthalene-1,3,6-trisulfonic acid (ANTS) (12.5 mM) was co-encapsulated with the cationic quencher p-xylene-bis-pyridinium bromide (DPX) (45 mM) into 100 nm large unilamellar vesicles (LUVs). BOK $\Delta$ C WT and D75R mutant were co-incubated with ANTS/DPX containing LUVs at different protein: lipid ratios. Liposome concentration used was 100  $\mu$ M. The leakage was followed in a SLM 8100 photon-counting spectrofluorometer (Spectronic Instrument, Rochester, NY, USA) using an excitation wavelength of 353 nm and an emission wavelength of 526 nm, both with 10 nm bandwidth slit. The fluorescence intensities were recorded as a function of time with 1 s intervals, setting the fluorescence at time t=0 to zero. The extent of marker release was quantified on a percentage basis according to the following equation: Leakage % =  $(F_t - F_0)/(F_{100} - F_0) \times 100$  where  $F_t$  is the measured fluorescence of protein-treated LUV at time t,  $F_0$  is the initial fluorescence of the LUV suspension before protein addition, and  $F_{100}$  is the fluorescence value after complete disruption of LUV by addition of TritonX-100 (final concentration of 0.25%).

# 3. RESULTS

## 3.1. MUTAGENESIS OF GST-BOK $\Delta$ C-6HIS

The sequence of BOK (UniProt entry Q9UMX3) was aligned to the sequences of its homologous pro-apoptotic relatives BAK (Q16611) and BAX (Q07812) using Clustal 2.1 multiple sequence alignment (**Figure 1A**). The  $\alpha$ -helices were assigned and the residues corresponding to the described salt-bridge were identified, from which mutants shown in **Figure 1.B** were designed. These two residues (D75

and K122) were mutated to their opposite charge, while trying to maintain the side-chain volume when possible in order to minimize structural changes.



**Figure 1. Sequential and structural analysis of human BOK and mutants.** (A) Amino acid sequence alignment of human BOK with homologous BAK and BAX (UniProt entries Q9UMX3, Q16611 and Q07812, respectively) specifying the mutated residues and the deleted 24 residues at its C-terminus corresponding to its transmembrane helical domain. (B) Homology model of BOKΔC24 using BCL-XLΔC (PDB entry 1G5) as a template highlighting the mutated residues represented in PyMol Viewer.

The BOK sequence used lacked the C-terminal 24 residues (called BOKΔC from this point on) corresponding to its transmembrane domain ( $\alpha 9$ ) to ease its manipulation in bacterial culture and subsequent purification steps. In addition, the BOKΔC construct was fused to GST followed by a PreScission protease cleavage site in its N-terminus in order to allow for affinity purification using reduced glutathione beads.

Mutants were generated by mutagenic PCR using the primers specified in **Methods Section 2.1**.

### 3.2. EXPRESSION OF RECOMBINANT GST- BOKΔC-6HIS

First of all, GST-BOKΔC-6His construct plasmid was inserted into DH5a *E. coli* competent cells via heat-shock induced transient pore formation to allow for plasmid amplification. Recombinant cells were selected by growth in ampicillin containing agar plates and medium, as gene conferring ampicillin resistance (*Amp<sup>r</sup>*) was included in the pGEX-3p-6 plasmid. In addition, selected colonies were checked for their mutations by sequencing. DNA was extracted and several *E. coli* strains transformed.

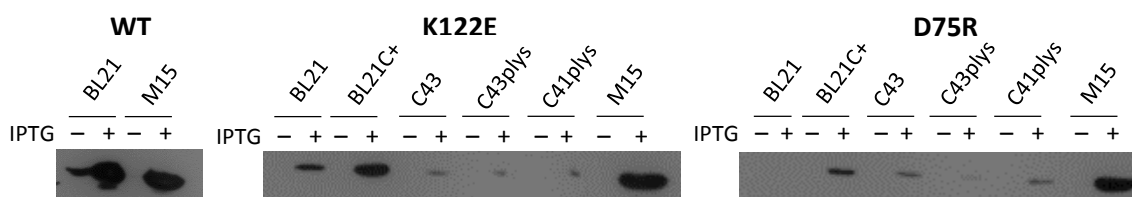


**Figure 2. WT, K122E and D75R BOK expression tests.** Indicated *E. coli* strains were transformed with WT and mutant GST-BOKΔC-6His (pGEX-6p-3 vector plasmid) and protein expression detected by Western blot analysis using anti-GST monoclonal antibody. Expression results before (-) and after (+) IPTG induction are shown.

Initially, *E. coli* BL21 strain was used for expression of GST-BOK $\Delta$ C-6His WT and mutants based on previous studies with WT BOK $\Delta$ C (19). However, this initial trial resulted in poor yield, most notably in the case of the mutants. Therefore, an expression test was performed in several *E. coli* strains (BL21, BL21C+, C43, C43plys, C41plys and M15) (**Figure 2**). This test was consistent with previous expression seen in BL21, with good expression of the WT protein –although a little leaky under no IPTG conditions–, poorer expression of K122E and no detectable expression of D75R. However, only two strains improved the yield of both mutants: BL21C+ and M15. M15 was selected for preparative expression showing the highest yield in mutants, as well as a good yield in the WT protein.

### 3.3. PURIFICATION OF GST-BOK $\Delta$ C-6HIS WT AND MUTANTS

GST-BOK $\Delta$ C-6His was first purified by affinity using reduced glutathione beads, which efficiently bind glutathione S-transferase protein (GST). The bacterial lysate supernatant coming from 6L culture of M15 *E. coli* strain was incubated with reduced glutathione beads, the mixture packed into a column and PreScission protease added (O/N incubation). 0.5 mL fractions were collected and loaded into a 10% SDS-PAGE gel for electrophoretic analysis by Coomassie blue staining (**Figure 3.I**).

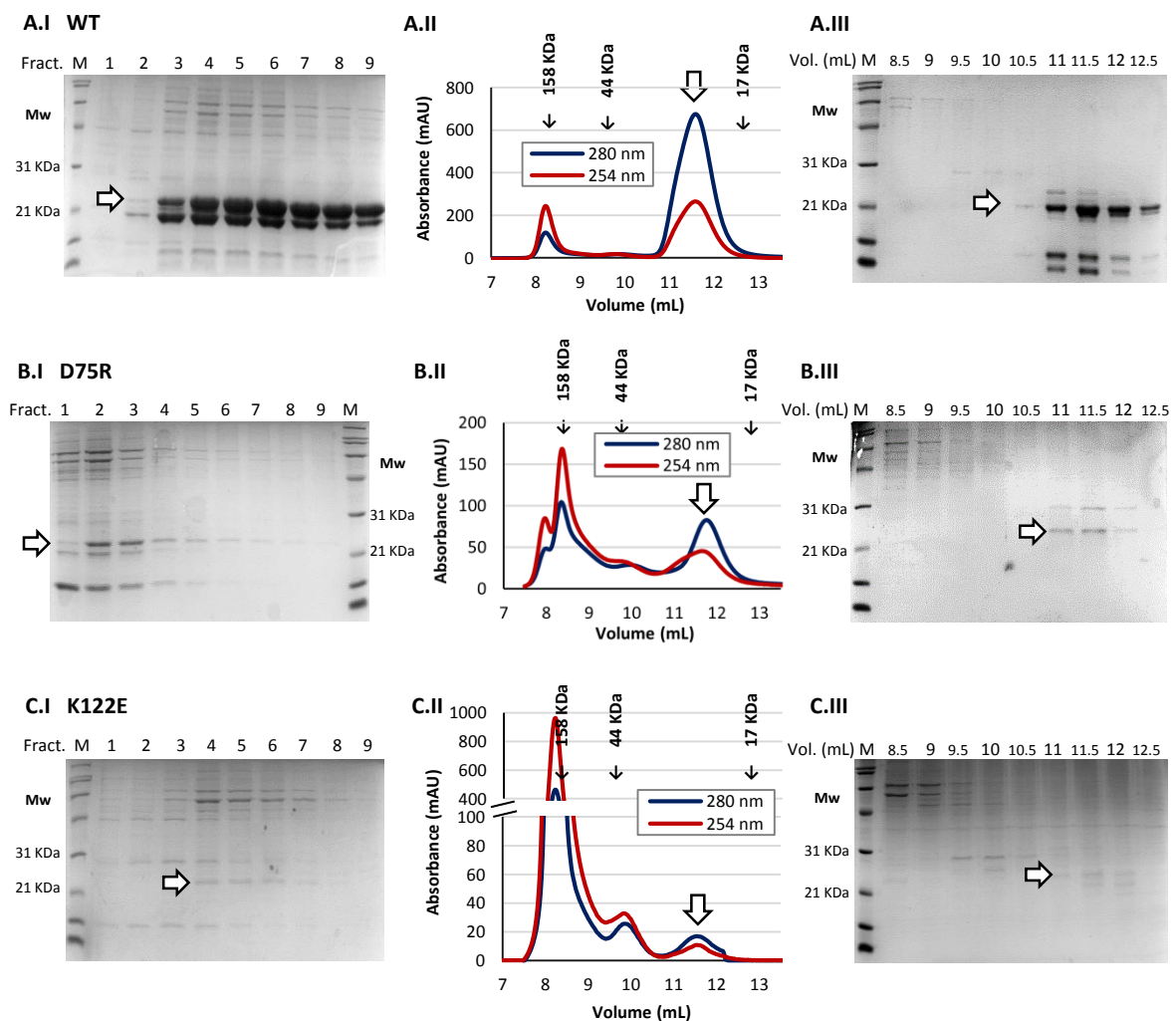


**Figure 3. Purification of GST-BOK $\Delta$ C-6His WT (A), D75R (B) and K122E (C) on M15 *E. coli* strain (6L).** (I) SDS-PAGE and Coomassie staining of the glutathione affinity purification after overnight incubation with PreScission protease (16h). Arrows indicate bands corresponding to BOK $\Delta$ C-6His. Chromatogram (II) and SDS-PAGE gel (III) from the size-exclusion chromatography of pooled fractions 3-8 from A.I, fractions 2-6 from B.I and 4-7 from C.I on a Superdex<sup>TM</sup> 75 column. In the chromatogram, absorbance at 280 and 254 nm are represented showing the first peak does not belong to a protein. The peaks and bands containing purified BOK $\Delta$ C-6His are indicated with an arrow.

In the first purification trial, most of the BOK $\Delta$ C-6His WT protein was lost in the pellet, which was concluded to be due to aggregation. Moreover, many degraded fractions were seen throughout the different purification steps (Not shown). Therefore, different elution conditions were tested in order to increase the final protein yield and quality. Based on a previous ThermoFluor<sup>®</sup> assay (19), two new buffers containing greater glycerol and salt content and with pH 8.0 and 6.0 instead of 7.5 were tried (Buffer A and Buffer B, **Methods section 2.5.1 and 2.5.2**). Resuspending GST- BOK $\Delta$ C-6His pellets in this new Buffer A (pH 8.0) in addition to eluting BOK $\Delta$ C-6His in Buffer B (pH 6.0) after incubation with PreScission protease showed greater protein stability, reflected in a reduction on degraded and aggregated fractions.

Optimized affinity purification of GST-BOK $\Delta$ C-6His showed the highest cleavage yield with intense bands through all fractions analysed by SDS-PAGE starting from fraction 3 (**Figure 3.A.I**). In this figure, two main bands appear, both of them belonging to BOK $\Delta$ C-6His, as concluded from Western blot analysis (Not shown). However, the band corresponding to full BOK $\Delta$ C-6His was concluded to be the top one (arrow) as deduced from its molecular mass of 21.7 KDa while the lower band was assumed to be a degraded fraction. In the case of the mutants, considerably lower yields were observed,

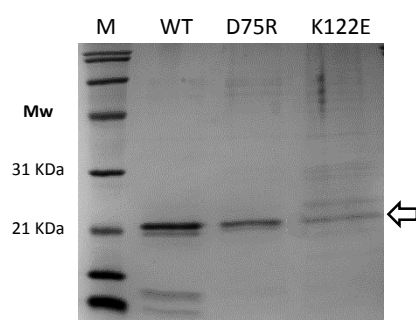


**Figure 4. Purified BOK $\Delta$ C-6His WT, D75R and K122E (10% SDS-PAGE).**

Both D75R and K122E were concentrated by TCA precipitation. All three BOK $\Delta$ C-6His variants were purified from an initial 6 L culture of M15 *E. coli* strain.

with most intense bands of BOK $\Delta$ C-6His corresponding to fractions 2 and 3 in the case of D75R mutant (**Figure 3.B.I**) and fractions 4 and 5 in the case of K122E mutant (**Figure 3.C.I**). In all three cases many other bands were observed, which probably corresponded to contaminants. Therefore, protein-containing fractions were pooled and loaded into a Superdex<sup>TM</sup> 75 column for a size-exclusion chromatography.

The resulting chromatogram and 10% SDS-PAGE of protein-containing fractions are showed in **Figure 3.II** and **III**. Chromatograms (**Figure 3.II**) show two main peaks: one around 8.25 mL and another one around 11.75 mL. The peak corresponding to BOK is the second one as the first peak was hypothesized to belong to DNA rather than to a protein due to its positive 254/280 absorbance ratio. All eluted BOK was hence concluded to be monomeric with the only peak around a molecular weight of 21 KDa. Once more, the chromatogram

of the WT protein showed the highest yield (**Figure 3.A.II**), followed by D75R (**Figure 3.B.II**) and K122E showing the lowest yield, with a peak under 20 mAU (note the different Y-axis scales). This is also seen in the SDS-PAGE of BOK $\Delta$ C-6His containing fractions (**Figure 3.III**), in which K122E is barely seen. In the case of the WT protein (**Figure 3.A.III**) the lower bands almost certainly correspond to degraded BOK $\Delta$ C-6His. In contrast, the upper bands seen in all chromatograms are probably contaminants. The resulting three purified proteins are shown in the SDS-PAGE gel in **Figure 4**. Both D75R and K122E were concentrated by TCA precipitation prior to gel electrophoresis. In the case of the WT protein, the two lower bands probably corresponding to degraded BOK $\Delta$ C-6His are seen once again. Either the obtained K122E final concentration or the total amount were remarkably lower than those of the WT protein and the D75R mutant, which made it impossible to use it for further studies. Thus, from this point on, all assays were performed with the WT protein and the D75R mutant of BOK $\Delta$ C-6His.

### 3.4. TRYPTOPHAN FLUORESCENCE ASSAYS

Tryptophan fluorescence is an easy way of monitoring protein general conformation and stability as its emission wavelength ranges from 300 to 350 nm depending on its microenvironment. BOK $\Delta$ C shows four Trp residues, three of which (W120, W164 and W171) seem to be buried into the inside of the protein and one (W50) sticking out at one of the sides, as predicted from a homology model using BCL-X $\Delta$ C (PDB entry 1G5) as a template (**Figure 5.A**). Therefore, Trp fluorescence of BOK $\Delta$ C can be used as an intrinsic probe to get a general idea of protein conformation in solution, without forgetting that the resulting emission wavelength will be an average from the four Trp's and their particular microenvironment.

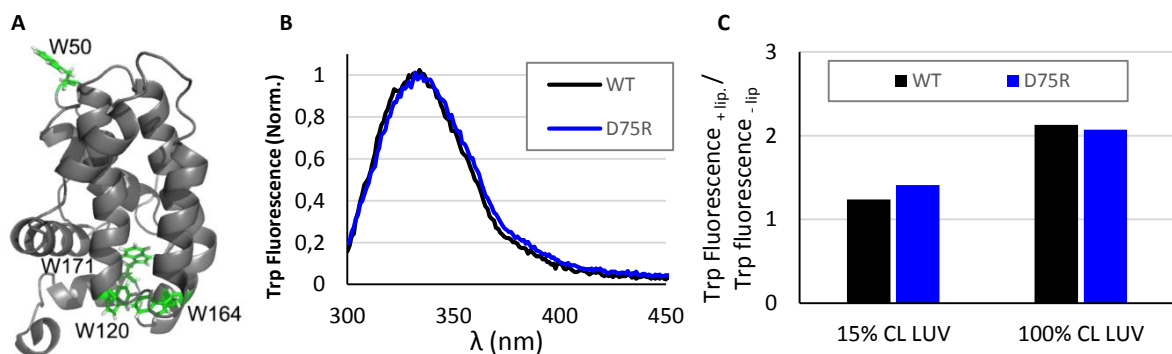


**Figure 5. Tryptophan fluorescence analysis of BOK $\Delta$ C-6His WT and D75R.** (A) Model of BOK $\Delta$ C showing its four Trp residues: W50, W120, W164 and W171 (PyMol Viewer). (B) Normalized tryptophan fluorescence analysis of the conformations of BOK $\Delta$ C-6His WT and D75R mutant in solution ( $\lambda_{\max} \approx 331$  nm). (C) Binding of BOK $\Delta$ C-6His WT and D75R to liposomes containing 15% and 100% cardiolipin (CL) (Trp fluorescence  $_{+liposome}$  / Trp fluorescence  $_{-liposome}$  ratio).

Both BOK $\Delta$ C-6His WT and D75R showed a similar tryptophan fluorescence spectra with a maximum wavelength of 331 nm (**Figure 5.B**), which indicates that both variants have roughly the same

conformation in solution. Fluorescence intensities were normalized to 1 to allow for better comparison of the maximum wavelength. In addition, the fluorescence ratio with to without liposomes ( $\text{Trp fluorescence}_{+\text{liposomes}} / \text{Trp fluorescence}_{-\text{liposomes}}$ ) was also measured (**Figure 5.C**). Both proteins bound 100% cardiolipin (CL) containing liposomes more readily than 15% CL containing liposomes, with a ratio of about 2 for 100% CL LUVs and a ratio of 1.25 for 15% CL LUVs. In either case, BOK $\Delta$ C-6His WT and D75R showed a similar binding ratio with respect to each other. In fact, despite D75R showing a slightly higher fluorescence ratio than the WT protein for 15% CL liposomes and slightly lower ratio for 100% CL liposomes, it cannot be stated from this experiment whether the difference seen was significant or not.

### 3.5. ANTS/DPX RELEASE FLUORESCENCE ASSAYS

Finally, BOK $\Delta$ C-6His WT and D75R were analysed for pore-forming activity in ANTS/DPX containing liposomes. Inside liposomes, the dye/quencher pair gets tightly packed showing all fluorescence quenched. However, when ANTS/DPX containing liposomes are co-incubated with a pore-forming protein that disrupts the continuity of the liposomal membrane, the liposomal contents are released resulting in ANTS fluorescence driven by dilution of both dye and quencher into surrounding medium. Thus, BOK $\Delta$ C-6His pore-forming activity can be monitored by measuring the increase in ANTS fluorescence intensity over time (**Figure 6.A**).

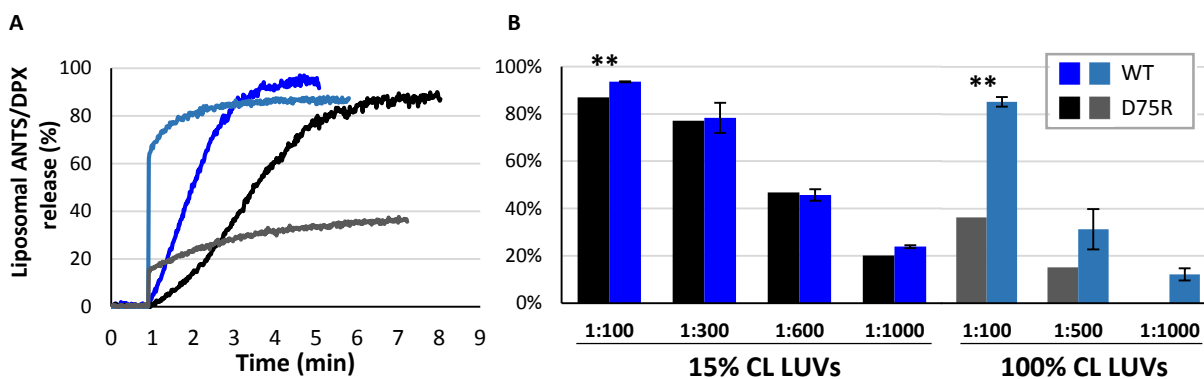


**Figure 6. ANTS/DPX liposome leakage fluorescence assay (% ANTS/DPX release).** (A) Representative kinetics of ANTS/DPX release elicited by BOK $\Delta$ C-6His WT and D75R in liposomes containing 15% and 100% CL at 1:100 protein:lipid ratio. (B) Average ANTS/DPX release for several protein:lipid ratios in 15% and 100% CL containing liposomes. As for D75R mutant, mean values  $\pm$  S.E. are shown for two independent replicates. Asterisks indicate significant differences as calculated from a Student t-test with a confidence level of 95%.

The initial ANTS/DPX release rate was greater for 100% CL liposomes than for 15% CL liposomes in both variants (**Figure 6.A**), according to what was seen for liposomal binding in **Figure 5.C**. In contrast, the total percentage of ANTS/DPX release was higher for 15% CL LUVs in all cases (**Figure 6.A and B**). Most remarkably, D75R mutant showed a higher initial rate of ANTS/DPX release than the WT protein for both 15% and for 100% CL containing LUVs (**Figure 6.A**), in stark contrast to what could have been expected. Furthermore, D75R mutant also showed higher total percentage of

ANTS/DPX release in almost all cases tested, despite just being statistically significant for 1:100 protein:lipid ratio (**Figure 6.B**).

## 4. DISCUSSION

Although carefully designed, D75R and K122E mutations seem to affect the stability of the protein, as both protein expression and purification yields were considerably lowered as compared to the WT protein. Even after the optimization of the expression system via the expression test and the improvement of the purification conditions, expression and purification of the mutants remained a challenge. In fact, one of the mutants (K122E) could not be obtained in sufficient amounts, so it had to be excluded in later experiments.

Despite the fact that D75R mutant also showed a lower yield and so that mutation probably hindered the right folding of the protein as well, the final purified protein obtained seemed to have similar conformation to the WT protein as shown by the Trp fluorescence spectra in **Figure 5.B**. Indeed, both the WT protein and the mutant showed almost superposed spectra with a maximum intensity wavelength of 331 nm in both cases. Therefore, the protein was concluded to be sufficiently stable and well folded to be relevant in subsequent studies.

As shown in **Figure 5.C**, both BOK $\Delta$ C-6His WT and D75R are capable of binding CL containing liposomes in a similar way. Moreover, both variants bind more readily to 100% CL LUVs than 15% CL LUVs, suggesting that the higher the CL content is, the easier BOK binds to liposomal membranes. This dependence on CL content suggests BOK binds to CL, which is consistent with previous studies (19). Taking into account that CL is particularly found in the mitochondria, this could indicate a role for BOK in mitochondrial apoptosis in addition to the role in the endoplasmic reticulum stress response that has been recently described (6,7).

ANTS/DPX assays revealed a higher initial rate for 100% CL containing liposomes in both the WT protein and the mutant (**Figure 6.A**). Together with the liposomal binding seen in **Figure 5.C**, a higher initial rate might support BOK's specificity for CL, binding more efficiently when the CL concentration is higher. In stark contrast, the total percentage of ANTS/DPX release was higher for 15% CL containing liposomes (**Figure 6.A and B**), which seems to contradict previous statements. However, it could be hypothesized that although a higher CL content would promote binding, too high CL concentration could actually be inhibitory with regard to pore-forming activity. As for this inhibition, two different options were regarded. On the one hand, too high CL concentrations could allow for a more rapid binding and insertion into the liposomal membrane but also for the formation of a more unstable pore that would disappear more quickly, whereas the pores in 15% CL LUVs would remain more stable in time. On the other hand, being a membrane solely composed by CL, the singular

membrane characteristics themselves could limit the pore size, thus limiting the amount of probe released when the difference in gradient gets reduced.

Most outstandingly, D75R mutant showed both a greater initial rate and a higher percentage of ANTS/DPX release in almost all conditions tested (**Figure 6.A and B**), which means an enhanced pore-forming activity as compared to the WT protein. This clearly contradicts the initial hypothesis, with this mutation not only having no effect on BOK's inherent pore-forming activity but also improving it. At first, it was believed to be an artefact resulting from the added positive charge that would more readily interact with the double negative charge of CL. However, this idea was not consistent with **Figure 5.C**, in which D75R mutant showed a similar tendency to bind 15% and 100% CL containing liposomes to that of the WT protein.

Another hypothesis that was considered was that D75R mutant could be less stable than the WT protein, supported by all the difficulties in expressing and purifying this variant. Thus, D75R would be more easily destabilized and therefore, adopt a more open conformation when inserted into liposomal membranes further promoting disruption of the membrane's integrity. Sadly, this would mean the results seen for this mutant have no real relevance when regarding BOK's oligomerization. Nevertheless, it should also be pointed out that this second hypothesis is not supported by the Trp fluorescence assay (**Figure 5.B**), in which the mutant BOK seemed to have a very similar conformation to the WT protein. However, Trp fluorescence is not a very accurate assay, and therefore the real conformational aberrations could get hidden.

On the other hand, it should be taken into account that these same mutations had already been generated in the homologous BAX and BAK and had been reported to abrogate dimerization as well as result in loss of function (10,12). In both BAX and BAK these mutations were representative of the proposed model, showing that they do follow the BH3-in-groove dimerization model and also, that this dimerization step is necessary for their pore-forming activity.

Thus, although the enhanced pore-forming activity seen in D75R mutant might well be an artefact, the fact that D75R mutant is still able to make a pore in liposomal models of the MOM must undoubtedly have some relevance. The results obtained here seem to indicate that BOK does not need to form a dimer in order to gain pore-forming activity and accomplish MOMP, or, at least, not the BH3-in-groove dimer described for BAX and BAK.

Any being the case, this study provides just a glimpse of BOK's activation mechanism and membrane activity and so, further experimental procedures such as a dimerization assay, as well as more accurate structural studies would be needed to have a better picture of BOK's real role in the mitochondrial outer membrane permeabilization. Not to mention studies with higher physiological relevance as could be using full mitochondria or directing studies in cellular models.

## 5. CONCLUDING REMARKS

This study supports the idea that BOK, unlike its pro-apoptotic relatives BAX and BAK and contrary to what was initially expected, does not follow the BH3-in-groove dimerization mechanism that had previously been described as an essential step for these proteins to gain pore-forming activity and undertake MOMP. Whether this means BOK differs from the other two BAX-like proteins in this functional aspect or that the dimerization is not really a pre-requisite but rather a consequence of the pore formation in the case of BAX and BAK is not fully clear yet, although previous studies of BAX and BAK seem to indicate that the first option is more probable. Why BOK would undergo a different mechanism to fulfil a similar function remains a mystery. In fact, there are still many questions that need to be answered in order to gain a better insight into BOK's role in the intricate network that composes mitochondrial apoptosis.

## 6. REFERENCES

1. Basañez G, Soane L, Hardwick JM. A New View of the Lethal Apoptotic Pore. *PLoS Biol.* 2012;10(9):9–12.
2. Czabotar PE, Lessene G, Strasser A, Adams JM. Control of apoptosis by the BCL-2 protein family: implications for physiology and therapy. *Nat Rev Mol Cell Biol.* Nature Publishing Group; 2014;15(1):49–63.
3. Hardwick JM, Chen Y, Jonas EA. Multipolar functions of BCL-2 proteins link energetics to apoptosis. *Trends Cell Biol.* 2012 Jun;22(6):318–28.
4. Youle RJ, Strasser A. The BCL-2 protein family: opposing activities that mediate cell death. *Nat Rev Mol Cell Biol.* 2008 Jan;9(1):47–59.
5. Tait SWG, Green DR. Mitochondria and cell death: outer membrane permeabilization and beyond. *Nat Rev Mol Cell Biol.* 2010 Sep;11(9):621–32.
6. Echeverry N, Bachmann D, Ke F, Strasser a, Simon HU, Kaufmann T. Intracellular localization of the BCL-2 family member BOK and functional implications. *Cell Death Differ.* 2013;20(6):785–99.
7. Carpio M a., Michaud M, Zhou W, Fisher JK, Walensky LD, Katz SG. BCL-2 family member BOK promotes apoptosis in response to endoplasmic reticulum stress. *Proc Natl Acad Sci U S A.* 2015;112(23):7201–6.
8. Hsu SY, Kaipia A, McGee E, Lomeli M, Hsueh AJ. Bok is a pro-apoptotic Bcl-2 protein with restricted expression in reproductive tissues and heterodimerizes with selective anti-apoptotic Bcl-2 family members. *Proc Natl Acad Sci U S A.* 1997 Nov 11;94(23):12401–6.

9. Beroukhi R, Mermel CH, Porter D, Wei G, Raychaudhuri S, Donovan J, et al. The landscape of somatic copy-number alteration across human cancers. *Nature*. 2010 Feb 18;463(7283):899–905.
10. Brouwer JM, Westphal D, Dewson G, Robin AY, Uren RT, Bartolo R, et al. Bak Core and Latch Domains Separate during Activation, and Freed Core Domains Form Symmetric Homodimers. *Mol Cell*. Elsevier Inc.; 2014;55(6):938–46.
11. Llambi F, Moldoveanu T, Tait SWG, Bouchier-Hayes L, Temirov J, McCormick LL, et al. A unified model of mammalian BCL-2 protein family interactions at the mitochondria. *Mol Cell*. 2011 Nov 18;44(4):517–31.
12. Czabotar PE, Westphal D, Dewson G, Ma S, Hockings C, Fairlie WD, et al. Bax crystal structures reveal how BH3 domains activate Bax and nucleate its oligomerization to induce apoptosis. *Cell*. 2013;152(3):519–31.
13. Dewson G, Ma S, Frederick P, Hockings C, Tan I, Kratina T, et al. Bax dimerizes via a symmetric BH3:groove interface during apoptosis. *Cell Death Differ*. 2012 Apr;19(4):661–70.
14. Bleicken S, Classen M, Padmavathi PVL, Ishikawa T, Zeth K, Steinhoff H-J, et al. Molecular details of Bax activation, oligomerization, and membrane insertion. *J Biol Chem*. 2010 Feb 26;285(9):6636–47.
15. Zhang Z, Zhu W, Lapolla SM, Miao Y, Shao Y, Falcone M, et al. Bax forms an oligomer via separate, yet interdependent, surfaces. *J Biol Chem*. 2010 Jun 4;285(23):17614–27.
16. Aluvila S, Mandal T, Hustedt E, Fajer P, Choe JY, Oh KJ. Organization of the mitochondrial apoptotic BAK pore: oligomerization of the BAK homodimers. *J Biol Chem*. 2014 Jan 31;289(5):2537–51.
17. Epand RF, Martinou J-C, Montessuit S, Epand RM. Transbilayer lipid diffusion promoted by Bax: implications for apoptosis. *Biochemistry*. 2003 Dec 16;42(49):14576–82.
18. Terrones O, Antonsson B, Yamaguchi H, Wang HG, Liu J, Lee RM, et al. Lipidic pore formation by the concerted action of proapoptotic BAX and tBID. *J Biol Chem*. 2004;279(29):30081–91.
19. Bustillo Zabalbeitia I. Membrane activities of Dynamin-Related Protein 1 (DRP1) and BCL2-related Ovarian Killer (BOK). Biophysics Unit (CSIC-UPV/EHU); 2015.